Engineering Structures 31 (2009) 2744–2755

Contents lists available at ScienceDirect

Engineering Structures

journal homepage: www.elsevier.com/locate/engstruct

Inelastic displacement ratios for SDOF structures subjected to repeated earthquakes

George D. Hatzigeorgiou [a,*], Dimitri E. Beskos [b,c]

[a] Department of Environmental Engineering, Democritus University of Thrace, GR-67100 Xanthi, Greece

[b] Department of Civil Engineering, University of Patras, GR-26500 Patras, Greece

[c] Office of Theoretical and Applied Mechanics, Academy of Athens, 4 Soranou Efessiou, GR-11527 Athens, Greece

ARTICLE INFO

Article history:
Received 18 March 2009
Received in revised form
1 June 2009
Accepted 2 July 2009
Available online 16 July 2009

Keywords:
Inelastic displacement ratios
Seismic analysis
Repeated earthquakes

ABSTRACT

Knowledge of the inelastic displacement ratio, i.e. the ratio of the maximum inelastic to the maximum elastic displacement of an SDOF system, allows the computation of its maximum inelastic displacement directly from the corresponding elastic one. This paper presents a simple and effective method for the inelastic displacement ratio estimation of a structure under repeated or multiple earthquakes. Extensive parametric studies are conducted to obtain expressions for this ratio, in terms of the period of vibration, the viscous damping ratio, the strain-hardening ratio, the force reduction factor and the soil class. It is found that the repeated earthquakes phenomenon has a significant effect on the inelastic displacement ratio and hence on the maximum inelastic displacement of SDOF systems.

© 2009 Elsevier Ltd. All rights reserved.

1. Introduction

In order to achieve the performance based seismic design demands for a structure, various methods of analysis are available. The most general and accurate method is three-dimensional (3-D) nonlinear time-history structural analysis. However, due to its complexity, simpler, yet trustworthy methods for estimating lateral inelastic displacement demands on structures are required not only for the design of new structures but also for the seismic evaluation and rehabilitation of existing structures. Such a method is static nonlinear or pushover analysis, which can determine the global force–displacement relationship of the structure, or capacity curve, in terms of the total lateral force (base shear) and the lateral deflection of the roof [1]. This capacity curve can then be transformed to a force–displacement relationship of a simplified single degree of freedom (SDOF) representation of the real multi degree of freedom (MDOF) structure. Pushover analysis can utilize a single or a multi mode lateral load or be associated with a modal approach [1–3]. The target roof displacement in all of these pushover procedures is determined from the maximum displacement of an inelastic SDOF system. This maximum displacement is also needed for the rapid seismic evaluation of existing buildings. Knowledge of the inelastic displacement ratio, i.e. the ratio of the maximum inelastic to the maximum elastic displacement of an SDOF system, allows the computation of its maximum inelastic displacement directly from the corresponding elastic one. Veletsos [4], Veletsos and Newmark [5] and Clough [6] observed that, according to the so-called 'equal-displacement rule', in the low frequency range of the spectrum the maximum displacement of an inelastic system may be considered the same as the maximum displacement of the associated elastic system, and thus knowledge of the maximum elastic displacement may provide a reasonable estimate of the inelastic one. However, Miranda [7], Decanini et al. [8], Ruiz-Garcia and Miranda [9,10] and Chopra and Chintanapakdee [11] showed that the inelastic displacement ratio can diverge significantly from unity in the moderately high to high frequency spectral regions. Recent investigations have shown that current standards used as the starting point for the seismic design of new structures, as well as of the seismic assessment of existing ones, can be significantly improved through an explicit account of lateral displacement demands [12–15]. The influence of various parameters on the inelastic displacement ratio is also examined in the abovementioned works. Thus, for example, Miranda and his co-workers [7,9,13] focused on the influence of site conditions, while Clough [6] and others [16,17] focused on the influence of the post-yield stiffness on the inelastic displacement ratio. In all the aforementioned investigations, the maximum displacement demands are based on the rare 'design earthquake' and the influence of repeated earthquake phenomena is ignored. To be sure, Amadio et al. [18] examined the effect of repeated earthquake ground motions on the nonlinear response of SDOF systems.

* Corresponding author. Tel.: +30 25410 79373; fax: +30 25410 79373.
E-mail address: gchatzig@env.duth.gr (G.D. Hatzigeorgiou).

0141-0296/$ – see front matter © 2009 Elsevier Ltd. All rights reserved.
doi:10.1016/j.engstruct.2009.07.002

However, as the authors themselves recognized, their work cannot be considered exhaustive since they examined only one natural and two artificial ground motions. Additionally, their seismic sequences seem to be notional since they were synthesized by two or three times the 'design earthquake'. Hatzigeorgiou [19] examined the influence of multiple earthquakes in numerous SDOF systems and found that seismic sequences lead to decreased force reduction factors in comparison with the case of the 'design earthquake'. However, that work is concerned with strength demands and not with displacements. The repeated earthquakes effect should not be confused with the low cycle fatigue phenomenon [20–23], which is referred to the importance of the plastic cycling effect and the accumulation of structural damage. This damage can only be indirectly related with the inelastic displacement ratio, is associated with the energy dissipation capacity and corresponds to single ground motions.

The main innovation of this paper is the development of a new procedure for the inelastic displacement ratio estimation of SDOF systems under multiple earthquakes, a phenomenon which has not studied in the past. Without loss of generality, elastic–plastic models with linear hardening or softening are adopted. These models are simple and can adequately describe steel or reinforced concrete structures with primarily flexural behavior. The influence of period of vibration, force reduction factor, site conditions, post-yield stiffness and damping is taken into account in constructing expressions for the inelastic displacement ratio through extensive parametric studies and nonlinear regression analysis. The maximum inelastic displacement is obtained by nonlinear dynamic time-history analysis. A statistical investigation of 5,644,800 inelastic time-history analyses is carried out to study 12,600 SDOF models excited by 112 earthquake accelerogram records from around the world, under 4 types of seismic sequence.

2. Description of model, seismic input and seismic sequence effect

An elastoplastic SDOF system with linear hardening or softening and viscous damping is used to model the structure, as shown in Fig. 1. The statistical dynamic response of this system to actual seismic records will be investigated in the next section. The dynamic equilibrium equation of an SDOF system is given by

$$m\ddot{u} + c\dot{u} + k^T u = -ma_g \tag{1}$$

where m is the mass, u the relative displacement, c the damping coefficient, k^T the tangent stiffness, and a_g the acceleration of the ground motion, while upper dots stand for time derivatives. If the required yield force for a system with available ductility μ is denoted by f_y and the maximum force response of the corresponding linear elastic system by f_{el} (Fig. 1), the force reduction factor R can be defined as

$$R = \frac{f_{el}}{f_y}. \tag{2}$$

Using traditional structural dynamics theory [24], SDOF systems are defined here by their elastic vibration period T, ranging from 0.1 s to 3.0 s, and viscous damping ratio ξ, assumed to be 1%, 2%, 5% and 10%. The yield force f_y can be expressed in terms of the yield displacement u_y and the elastic stiffness k_{el} as

$$f_y = k_{el} \cdot u_y \tag{3}$$

while the ductility μ is defined in terms of the maximum displacement $u_{\max}$ and the yield displacement u_y, as

$$\mu = \frac{u_{\max}}{u_y}. \tag{4}$$

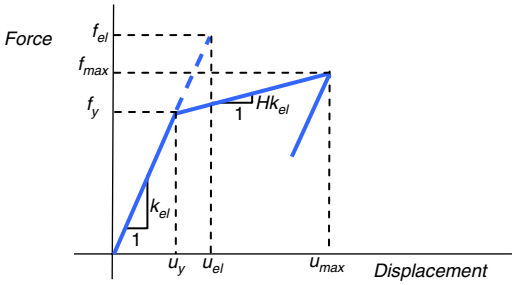

Fig. 1. Bilinear elastoplastic model of an SDOF.

Strain hardening or softening takes place after yielding initiates. The tangent stiffness is defined as the slope $k_t = H \cdot k_{el}$ of the second branch of the skeleton force–displacement relationship (Fig. 1). In this work seven different values of the post-yield stiffness ratio, $H = k_t/k_{el}$, are examined. These are 0%, which corresponds to an elastic–perfectly plastic model, 1%, 3% and 5% for the linear hardening model, and −1%, −3% and −5% for the linear softening model. Unloadings and subsequent loadings are assumed to be parallel to the original loading curve, as shown in Fig. 1.

Finally, the inelastic displacement ratio is defined as the maximum lateral inelastic displacement $u_{\max}$ divided by the maximum lateral elastic displacement u_{el} for a system with the same mass and initial stiffness (i.e., same period of vibration) subjected to the same earthquake ground motion. This ratio is given by

$$IDR = \frac{u_{\max}}{u_{el}} = \frac{\mu}{R}. \tag{5}$$

A total of 112 real earthquake acceleration time-histories from around the world are used in this study. These accelerograms present maximum ground acceleration greater or equal to 0.10g and are recorded at sites ranging from hard rock to soft soil conditions according to the definitions of the United States Geological Survey (USGS) site classification system [25]. More specifically, 4 groups of 28 accelerograms are examined, which correspond to:

- hard rock site conditions with shear wave velocity 750 m/s $\leq V_S$ (soil type A).
- soft rock or very dense soil with shear wave velocity 360 m/s $\leq V_S <$ 750 m/s (soil type B)
- stiff soil with shear wave velocity 180 m/s $\leq V_S <$ 360 m/s (soil type C)
- soft soil with shear wave velocity 180 m/s $> V_S$ (soil type D).

The complete list of these earthquakes, which was downloaded from the strong motion database of the Pacific Earthquake Engineering Research (PEER) Center [26], is shown in Tables 1–4. The total sample of earthquakes can be characterized as fairly broad since it ranges in terms of maximum ground acceleration between 98 and 806 cm/s^2, i.e., between 0.100g and 0.822g. The mean response elastic spectra ($\xi = 5\%$) for the four aforementioned groups and the whole sample are presented in Fig. 2. These spectra seem to be similar to the corresponding design spectra proposed by modern seismic codes with analogous site classification systems. Furthermore, this soil classification system is quite similar to EC8 provisions [27] since the only difference between the EC8 and USGS categorizations has to do with the characteristic shear wave velocity of hard rock, which is greater than or equal to 800 m/s and 750 m/s, respectively.

The central difference method is used here for the dynamic analysis of elastoplastic SDOF systems to avoid numerical–artificial damping. Generally, the analysis time step is a small portion, equal to 1/10 in this study, of the sampling time of the digitized earthquake record, to satisfy the following criteria [24]: (i) the

Table 1
Recorded earthquake ground motions which correspond to soil type A.

No.	Date	Record name	Comp.	Station name	*PGA* (*g*)
1	1986/07/08	N. Palm Springs	EW	5224 Anza	0.104
2	1989/10/18	Loma Prieta	N205	58539 San Francisco	0.105
3	1999/09/20	Chi-Chi, Taiwan	056-N	HWA056	0.107
4	1999/09/20	Chi-Chi, Taiwan	056-N	HWA056	0.107
5	1994/01/17	Northridge	N175	90017 LA-Wonderland Ave	0.112
6	1986/07/08	N. Palm Springs	EW	12206 Silent Valley	0.113
7	1975/06/07	Northern Calif	N060	1249 Cape Mendocino, Petrolia	0.115
8	1992/06/28	Landers	NS	21081 Amboy	0.115
9	1999/09/20	Chi-Chi, Taiwan	EW	TAP103	0.122
10	1987/10/01	Whittier Narrows	EW	24399 Mt Wilson-CIT Station	0.123
11	1986/07/08	N. Palm Springs	NS	5224 Anza	0.129
12	1999/09/20	Chi-Chi, Taiwan	N034	TCU046	0.133
13	1971/02/09	San Fernando	N159	127 Lake Hughes #9	0.134
14	1999/08/17	Kocaeli, Turkey	NS	Gebze	0.137
15	1986/07/08	N. Palm Springs	NS	12206 Silent Valley	0.139
16	1994/01/17	Northridge	EW	90019 San Gabriel-E. Gr. Ave.	0.141
17	1987/10/04	Whittier Narrows	EW	24399 Mt Wilson-CIT Station	0.142
18	1992/06/28	Landers	EW	21081 Amboy	0.146
19	1971/02/09	San Fernando	N069	127 Lake Hughes #9	0.157
20	1987/10/04	Whittier Narrows	NS	24399 Mt Wilson-CIT Station	0.158
21	1994/01/17	Northridge	N005	90017 LA-Wonderland Ave	0.172
22	1999/09/20	Chi-Chi, Taiwan	NS	TAP103	0.177
23	1975/06/07	Northern Calif	N150	1249 Cape Mendocino, Petrolia	0.179
24	1987/10/01	Whittier Narrows	NS	24399 Mt Wilson-CIT Station	0.186
25	1999/08/17	Kocaeli, Turkey	EW	Gebze	0.244
26	1994/01/17	Northridge	NS	90019 San Gabriel-E. Gr. Ave.	0.256
27	1989/10/18	Loma Prieta	EW	47379 Gilroy Array #1	0.411
28	1989/10/18	Loma Prieta	NS	47379 Gilroy Array #1	0.473

Table 2
Recorded earthquake ground motions which correspond to soil type B.

No.	Date	Record name	Comp.	Station name	*PGA* (*g*)
1	1978/08/13	Santa Barbara	N138	283 Santa Barbara Courthouse	0.102
2	1979/08/06	Coyote Lake	N303	1377 San Juan Bautista	0.107
3	1979/08/06	Coyote Lake	N213	1377 San Juan Bautista	0.108
4	1980/01/27	Livermore	EW	67070 Antioch- %10 G St	0.112
5	1992/04/25	Cape Mendocino	NS	89509 Eureka	0.154
6	1979/10/15	Imperial Valley	N237	6604 Cerro Prieto	0.157
7	1970/09/12	Lytle Creek	N115	290 Wrightwood	0.162
8	1979/10/15	Imperial Valley	N147	6604 Cerro Prieto	0.169
9	1992/04/25	Cape Mendocino	EW	89509 Eureka	0.178
10	1970/09/12	Lytle Creek	N205	290 Wrightwood	0.200
11	1978/08/13	Santa Barbara	N048	283 Santa Barbara Courthouse	0.203
12	1976/09/15	Friuli, Italy	NS	8014 Forgaria Cornino	0.212
13	1986/07/08	N. Palm Springs	NS	12204 San Jacinto-Soboba	0.239
14	1986/07/08	N. Palm Springs	EW	12204 San Jacinto-Soboba	0.250
15	1976/09/15	Friuli, Italy	EW	8014 Forgaria Cornino	0.260
16	1992/06/28	Landers	EW	22170 Joshua Tree	0.274
17	1992/06/28	Landers	NS	22170 Joshua Tree	0.284
18	1989/10/18	Loma Prieta	NS	58065 Saratoga-Aloha Ave	0.324
19	1994/01/17	Northridge	NS	90021 LA-N Westmoreland	0.361
20	1999/09/20	Chi-Chi, Taiwan	NS	TCU095	0.378
21	1992/04/25	Cape Mendocino	EW	89324 Rio Dell Overpass	0.385
22	1994/01/17	Northridge	EW	90021 LA-N Westmoreland	0.401
23	1989/10/18	Loma Prieta	EW	58065 Saratoga-Aloha Ave	0.512
24	1999/09/20	Chi-Chi, Taiwan	N045	TCU045	0.512
25	1992/04/25	Cape Mendocino	NS	89324 Rio Dell Overpass	0.549
26	1980/06/09	Victoria, Mexico	N135	6604 Cerro Prieto	0.587
27	1980/06/09	Victoria, Mexico	N045	6604 Cerro Prieto	0.621
28	1999/09/20	Chi-Chi, Taiwan	NS	TCU095	0.712

adopted time step should not exceed 1/10 of the minimum natural vibration period of the system and (ii) the adopted time step should be much less than the totally minimum period corresponding to the several main frequency components of the earthquake record.

This work examines the influence of multiple earthquakes. This investigation is vital for the satisfaction of the principles of performance-based seismic design associated with structural damage and collapse. As is expected, the deformation demand required by multiple seismic ground motions can be notably higher than that required by a single event [28]. Earthquake sequences are characterized by the reappearance of medium or strong seismic ground motions after short or long periods of time. For example, according to PEER database [26], the 46T04CHP station recorded the Coalinga earthquake (1983/07/22, 02:39), a large seismic motion ($M_L = 6.0$) with peak ground acceleration equal to $0.605g$. After a few days (1983/07/25, 22:31), the same station and in the same direction recorded another earthquake with smaller magnitude ($M_L = 5.3$) than the previous one. However, the second event presented higher peak ground acceleration, equal to $0.733g$. The corresponding response spectra for $\xi = 5\%$ appear in Fig. 3(a). It is evident that in spite of the lower magnitude, the spectrum of the second earthquake (1983/07/25)

Table 3
Recorded earthquake ground motions which correspond to soil type C.

No.	Date	Record name	Comp.	Station name	*PGA* (*g*)
1	1999/08/17	Kocaeli, Turkey	NS	Atakoy	0.105
2	1968/04/09	Borrego Mtn	NS	117 El Centro #9	0.130
3	1983/05/02	Coalinga	NS	36227 Parkfield	0.131
4	1979/10/15	Imperial Valley	N285	6622 Compuertas	0.147
5	1983/05/02	Coalinga	EW	36227 Parkfield	0.147
6	1989/10/18	Loma Prieta	EW	57066 Agnes State Hospital	0.159
7	1999/08/17	Kocaeli, Turkey	EW	Atakoy	0.164
8	1989/10/18	Loma Prieta	NS	57066 Agnes State Hospital	0.172
9	1971/02/09	San Fernando	NS	135 LA-Hollywood	0.174
10	1979/10/15	Imperial Valley	N015	6622 Compuertas	0.186
11	1971/02/09	San Fernando	EW	135 LA-Hollywood	0.210
12	1989/10/18	Loma Prieta	EW	1028 Hollister City Hall	0.215
13	1984/04/24	Morgan Hill	NS	57382 Gilroy Array #4	0.224
14	1989/10/18	Loma Prieta	NS	1028 Hollister City Hall	0.247
15	1987/11/24	Superstitn Hills-B	NS	01335 El Centro Imp. Co. Cent	0.258
16	1979/10/15	Imperial Valley	N012	6621 Chihuahua	0.270
17	1979/10/15	Imperial Valley	N282	6621 Chihuahua	0.284
18	1980/01/27	Livermore	EW	57187 San Ramon	0.301
19	1999/09/20	Chi-Chi, Taiwan	EW	NST	0.309
20	1984/04/24	Morgan Hill	EW	57382 Gilroy Array #4	0.348
21	1987/11/24	Superstitn Hills-B	EW	01335 El Centro Imp. Co. Cent	0.358
22	1981/04/26	Westmorland	NS	5169 Westmorland Fire Sta	0.368
23	1999/09/20	Chi-Chi, Taiwan	NS	NST	0.388
24	1994/01/17	Northridge	EW	90057 Canyon Country	0.410
25	1994/01/17	Northridge	NS	90057 Canyon Country	0.482
26	1981/04/26	Westmorland	EW	5169 Westmorland Fire Sta	0.496
27	1999/11/12	Duzce, Turkey	NS	Bolu	0.728
28	1999/11/12	Duzce, Turkey	EW	Bolu	0.822

Table 4
Recorded earthquake ground motions which correspond to soil type D.

No.	Date	Record name	Comp.	Station name	*PGA* (*g*)
1	1989/10/18	Loma Prieta	EW	58117 Treasure Island	0.100
2	1999/09/20	Chi-Chi, Taiwan	NS	TAP003	0.106
3	1979/10/15	Imperial Valley	N040	5057 El Centro Array #3	0.112
4	1987/11/24	Superstitn Hills	N045	5062 Salton Sea Wildlife Refuge	0.119
5	1999/09/20	Chi-Chi, Taiwan	N040	TCU040	0.123
6	1999/09/20	Chi-Chi, Taiwan	EW	TAP003	0.126
7	1994/01/17	Northridge	N064	90011 Montebello-Bluff Rd.	0.128
8	1999/09/20	Chi-Chi, Taiwan	N130	TCU040	0.149
9	1989/10/18	Loma Prieta	NS	58117 Treasure Island	0.159
10	1987/11/24	Superstitn Hills	N135	5062 Salton Sea WildlifeRefuge	0.167
11	1981/04/26	Westmorland	N135	5062 Salton Sea Wildlife Ref.	0.176
12	1994/01/17	Northridge	N154	90011 Montebello-Bluff Rd.	0.179
13	1979/10/15	Imperial Valley	N130	5057 El Centro Array #3	0.179
14	1999/08/17	Kocaeli, Turkey	NS	Ambarli	0.184
15	1981/04/26	Westmorland	N045	5062 Salton Sea Wildlife Ref.	0.199
16	1995/01/16	Kobe	EW	0-Shin-Osaka	0.212
17	1989/10/18	Loma Prieta	N133	1002 APEEL 2-Redwood City	0.220
18	1989/10/18	Loma Prieta	N137	1002 APEEL 2-Redwood City	0.220
19	1995/01/16	Kobe	NS	0-Shin-Osaka	0.243
20	1999/08/17	Kocaeli, Turkey	EW	Ambarli	0.249
21	1995/01/16	Kobe	NS	Kakogawa	0.251
22	1989/10/18	Loma Prieta	N043	1002 APEEL 2-Redwood City	0.274
23	1989/10/18	Loma Prieta	N047	1002 APEEL 2-Redwood City	0.274
24	1999/09/20	Chi-Chi, Taiwan	N131	CHY041	0.302
25	1995/01/16	Kobe	EW	Kakogawa	0.345
26	1995/01/16	Kobe	NS	Nishi-Akashi	0.503
27	1995/01/16	Kobe	EW	Nishi-Akashi	0.509
28	1999/09/20	Chi-Chi, Taiwan	N041	CHY041	0.639

almost covers the corresponding spectrum of the former seismic event (1983/07/22) and, for this reason, is almost identical to the 'total' elastic spectrum of seismic sequence (1983/07/22 + 25). This is a typical example of a real seismic sequence. It should be noted that the majority of ground motions have medium or strong foreshocks and/or aftershocks. Fig. 3(b) also shows the inelastic displacement ratios for $R = 5$ and $H = -3\%$, for the single seismic events and the seismic sequence. It is obvious that the latter case leads to noticeably increased inelastic displacement ratios in comparison with the single events, despite the almost identical elastic spectra of the second event and the seismic sequence. Generally, the increase of deformation demands, which can be directly related to local or global damage, depends on the characteristics of the seismic motions. However, the examination of an adequate number of seismic events reduces the influence of these characteristics. In this work, each of the 112 aforementioned seismic records is applied one, two and three times, which are noted in the following as *Case* 1, *Case* 2 and *Case* 3, respectively. As a typical example, Fig. 4 shows the adopted sequence hypothesis for the Kobe earthquake (1995/01/16). Between two consecutive seismic events a time gap is applied, which is equal to three times the single event duration. This gap is absolutely enough

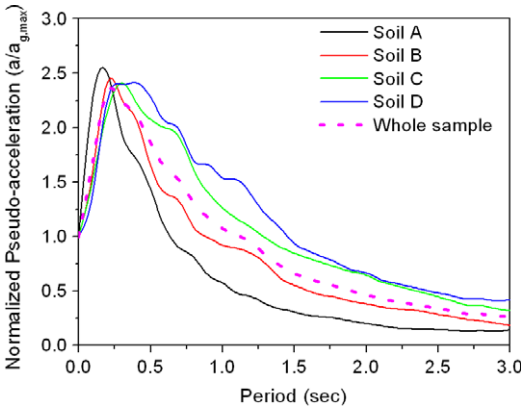

Fig. 2. Acceleration spectra for the four groups of accelerograms.

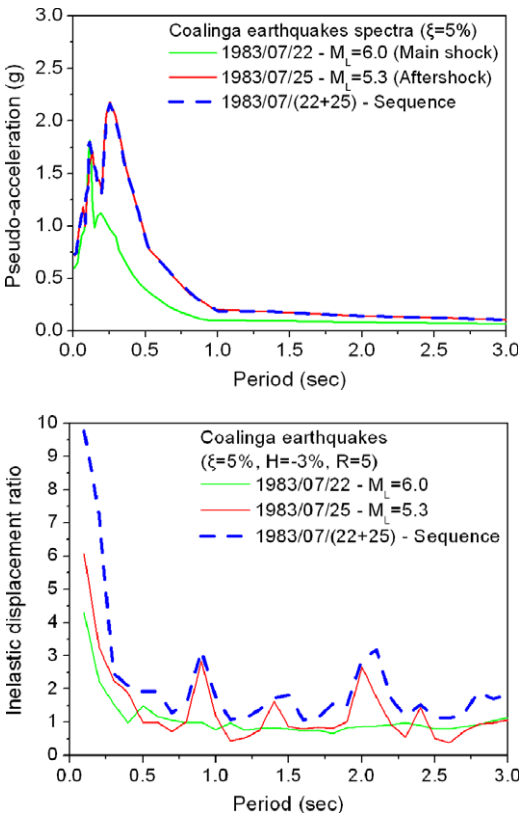

Fig. 3. The Coalinga earthquake: Response and inelastic displacement ratio spectra.

to cease the moving of any structure due to damping. Therefore, the total duration for a set of two and three earthquakes is equal to 5 and 9 times the single event duration, respectively. It should be noted that the elastic spectra of the aforementioned groups of accelerograms (Fig. 2) are absolutely identical for single, double and triple excitations. Real sequences of seismic events are not examined in this paper since they present dissimilar characteristics, making the analysis extremely complex and not leading to transpicuous and practically useful conclusions. In addition, another seismic sequence combination, which is noted in the following as *Case* 4, is examined. This is based on the well-known Gutenberg–Richter law [29], which expresses the relationship between the magnitude and total number of earthquakes in any given region and time period, which can be written as

$$N = 10^{A-BM} \tag{6}$$

where N is the number of events in a given magnitude range, M the magnitude range and A and B are constants, with the first one indicating the total seismicity rate of the examined region and the second one being typically equal to 1.0. This means that for every event with magnitude M there will be two earthquakes with magnitude $(M - 0.3010)$ and three earthquakes with magnitude $(M - 0.4771)$, since $\log(2) \cong 0.3010$ and $\log(3) \cong 0.4771$. For example, for every ground motion with $M = 7.0$, there will be two earthquakes with magnitude $M = 7.0000 - 0.3010 \cong 6.7$ and three earthquakes with $M = 7.0000 - 0.4771 \cong 6.5$. These magnitudes can be characterized as contiguous, and therefore can be derived from a specific fault. Thus, as Chouhan and Srivastava [30] noted, there is no difference in the values of the abovementioned parameter B obtained for the foreshock or aftershock sequences and the main shock of the same region. Furthermore, there are many research works which relate the magnitude of an earthquake with the expected horizontal peak ground acceleration (PGA). Without loss of generality, the well-known Joyner–Boore [31] empirical relation, based on Western US and worldwide records, is adopted herein in the form

$$\log(PGA) = 0.49 + 0.23(M - 6) - \log\sqrt{R^2 + 8^2} - 0.0027\sqrt{R^2 + 8^2} \tag{7}$$

where the PGA is expressed in terms of gravitational acceleration g, and the source distance R is given in km.

According to Eqs. (6) and (7), irrespective of the source distance and earthquake magnitude, the ratios between the peak ground accelerations for the aforementioned cases are given by

$$\begin{aligned}\frac{PGA_{(2\text{-}EVENTS)}}{PGA_{(1\text{-}EVENT)}} &= \frac{PGA_{M-0.3010}}{PGA_M} \\ &= \frac{10^{.49+0.23(M-0.3010-6)-\log\sqrt{R^2+8^2}-0.0027\sqrt{R^2+8^2}}}{10^{.49+0.23(M-6)-\log\sqrt{R^2+8^2}-0.0027\sqrt{R^2+8^2}}} \\ &= 10^{-0.23\cdot 0.3010} = 0.8526\end{aligned} \tag{8}$$

$$\begin{aligned}\frac{PGA_{(3\text{-}EVENTS)}}{PGA_{(1\text{-}EVENT)}} &= \frac{PGA_{M-0.4771}}{PGA_M} \\ &= \frac{10^{.49+0.23(M-0.4771-6)-\log\sqrt{R^2+8^2}-0.0027\sqrt{R^2+8^2}}}{10^{.49+0.23(M-6)-\log\sqrt{R^2+8^2}-0.0027\sqrt{R^2+8^2}}} \\ &= 10^{-0.23\cdot 0.4771} = 0.7767.\end{aligned} \tag{9}$$

This means that for every seismic event with PGA equal to $A_{g,\max}$, there will be two earthquakes with PGA equal to $0.8526 \cdot A_{g,\max}$ and three earthquakes with PGA equal to $0.7767 \cdot A_{g,\max}$. As explained above, these events can be derived from a specific fault. In reality, structures can be subjected to any possible combination of the above events. In this paper, the following rational combination of the aforementioned cases is examined: 1 seismic event $(A_{g,\max}) + 2$ seismic events $(0.8526 \cdot A_{g,\max})$. This assumption is considered to represent *Case* 4 where, without loss of generality, the two smaller events precede and follow the bigger one. Thus, assuming that these events appear in a short period of time, they can be characterized as the *foreshock* and the *aftershock*, while the medial is characterized as the as the *main shock*.

Cases 1 to 4 can be generally considered as triple earthquakes, where every one of their three discrete parts is multiplied with appropriate factors as:

- *Case* 1: (1.0000, 0.0000, 0.0000), as shown in Fig. 4(a),
- *Case* 2: (1.0000, 1.0000, 0.0000), as shown in Fig. 4(b),
- *Case* 3: (1.0000, 1.0000, 1.0000), as shown in Fig. 4(c),
- *Case* 4: (0.8526, 1.0000, 0.8526), as shown in Fig. 4(d).

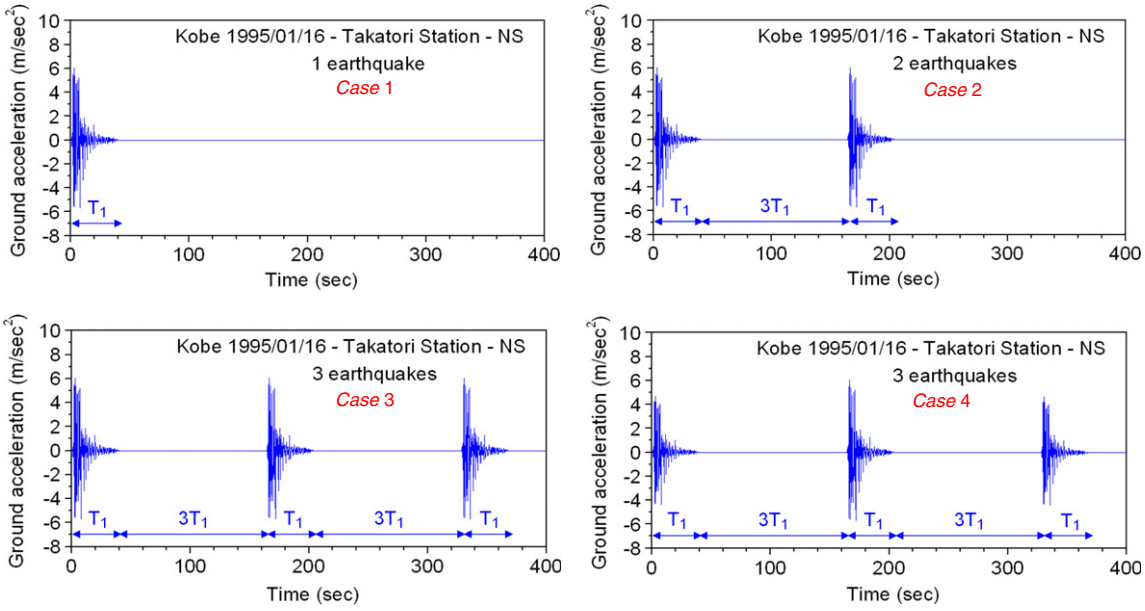

Fig. 4. Typical examples of a seismic sequence: *Cases* 1–4.

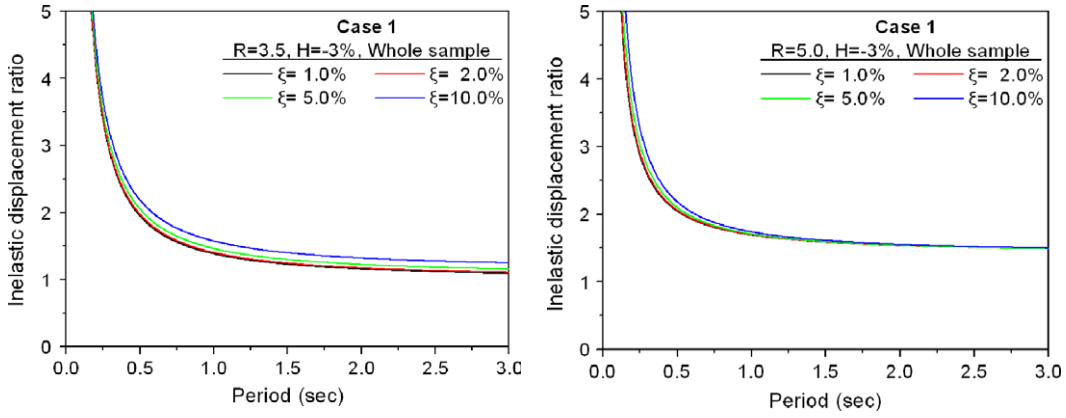

Fig. 5. Influence of viscous damping ratio.

It should be noted that according to *Cases* 2–4, if a structure has already been damaged during the first seismic event and not yet repaired, it may become totally inadequate at the end of the seismic sequence. For each earthquake record, the period of the SDOF system is increased from 0.1 to 3.0 s with an increment of 0.1 s (i.e., 30 values of period), while the force reduction factor is assumed to increase from 1.0 to 8.0 with an increment of 0.5 (i.e., 15 values of R factors). Thus, 5,644,800 analyses are examined: (112 ground motions) × (4 cases of seismic sequence) × (30 periods, T) × (4 viscous damping ratios, ξ) × (7 post-elastic stiffness ratios, H) × (15 force reduction factor, R). Every analysis serves to solve the nonlinear differential equation (1) by the aforementioned central difference method and determine the response $u(t)$ in terms of various parameters of the problem (T, ξ, H, R, soil type and seismic sequence).

3. Proposed empirical expressions for the inelastic displacement ratio

A complete nonlinear regression analysis is carried out on the basis of the data obtained by the aforementioned response analyses. The relation of the inelastic displacement ratio versus the structural period and force reduction factor is regressed for the series of the aforementioned 5,644,800 analyses in such a way so that the effect of viscous damping ratio and the post-elastic stiffness ratio as well as the soil type and the case of seismic sequence to be also taken into account in the resulting expression. Thus, the following empirical expression for the inelastic displacement ratio T–R–ξ–H is obtained for the firm sites and the seismic sequence under consideration:

$$\text{Inelastic displacement ratio}\,(T, R) = 1 + a\left(\frac{R-1}{R}\right)\left(T^b + R^c + d\right). \tag{10}$$

In Eq. (10), a, b, c and d are coefficients which take into account the influence of viscous damping ratio, ξ, post-yield stiffness ratio, H, soil type and seismic sequence where one, two and three earthquakes are considered (*Cases* 1–4). In this work, the aforementioned coefficients are given by the following empirical expressions:

$$a(\xi, H) = a_1 + a_2\xi + a_3H + a_4H^2 \tag{11}$$

$$b(\xi, H) = b_1 + b_2\xi + b_3H + b_4H^2 \tag{12}$$

$$c(\xi, H) = c_1 + c_2\xi + c_3H + c_4H^2 \tag{13}$$

$$d(\xi, H) = d_1 + d_2\xi + d_3H + d_4H^2. \tag{14}$$

The coefficients a_i, b_i, c_i and d_i (i = 1–4) are summarized in Table 5 for the firm sites and the seismic sequence under consideration.

Table 5
Coefficients a_i, b_i, c_i and d_i ($i = 1$–4).

Soil type	Parameter	1	2	3	4	r^2
Case 1—1 earthquake (1.0000, 0.0000, 0.0000)						
A	a	0.096847	0.543074	−2.73182	179.327	0.9883
	b	−1.48148	−0.878420	−3.47869	217.881	
	c	0.769098	−1.75128	−3.88837	−96.1181	
	d	−2.21646	6.93376	−1.59369	87.6535	
B	a	0.129385	0.589640	−3.37800	282.736	0.9882
	b	−1.69337	0.624392	−3.00606	263.431	
	c	0.568195	−0.457730	−7.26905	−136.354	
	d	−2.63578	5.45507	3.41175	249.402	
C	a	0.488390	0.330289	−9.61847	142.252	0.9825
	b	−1.24221	−0.547800	−5.51635	−19.4654	
	c	0.472032	−0.440450	−2.15621	4.98701	
	d	−2.49009	4.81703	−2.89469	67.5202	
D	a	0.128233	0.878371	−4.11900	246.914	0.9784
	b	−1.95993	1.22806	−3.45501	240.679	
	c	0.723390	−1.20677	−3.88315	−120.473	
	d	−2.63519	8.59840	−5.27300	215.581	
Whole sample	a	0.151448	0.810737	−5.03997	247.425	0.9723
	b	−1.66784	0.458836	−4.62420	237.541	
	c	0.647908	−1.02127	−3.90981	−88.3191	
	d	−2.54472	6.32121	−0.952320	148.149	
Case 2—2 earthquakes (1.0000, 1.0000, 0.0000)						
A	a	0.259060	1.13879	−6.67583	266.905	0.9858
	b	−1.19772	−0.344690	−6.27206	173.378	
	c	0.330504	−2.67848	−17.6917	−379.953	
	d	0.419858	1.69680	−6.98372	−138.645	
B	a	0.215845	2.21847	−7.12891	368.556	0.9881
	b	−1.55708	2.18173	−6.37215	243.493	
	c	0.365700	−1.84694	−20.5463	−411.860	
	d	−0.532740	3.53160	−4.90516	2.87810	
C	a	0.909223	0.617089	−22.1784	169.221	0.9803
	b	−1.04172	−0.004580	−13.0356	−115.553	
	c	0.173897	−0.939680	−18.6708	−316.066	
	d	−1.31581	4.15598	9.87709	376.106	
D	a	0.191651	2.05739	−5.82608	282.166	0.9802
	b	−1.83214	2.71589	−6.70607	227.482	
	c	0.195246	−2.94461	−36.8408	−757.132	
	d	0.397083	3.73826	−17.2439	−43.9822	
Whole sample	a	0.249705	1.90889	−7.24062	285.976	0.9756
	b	−1.54313	1.64267	−7.20201	214.110	
	c	0.321272	−2.20950	−22.9385	−453.669	
	d	−0.115070	3.03502	−7.72518	−12.5433	
Case 3—3 earthquakes (1.0000, 1.0000, 1.0000)						
A	a	2.43813	1.32535	−75.6037	757.741	0.9745
	b	−0.297160	−0.593140	−11.2864	−115.961	
	c	−0.136130	−1.16386	−14.5777	−315.233	
	d	−1.10803	1.17481	12.4892	241.126	
B	a	0.552181	4.53541	−18.4852	578.975	0.9719
	b	−1.13782	2.13948	−8.10458	169.993	
	c	0.028773	−2.21949	−23.6018	−551.496	
	d	−0.083870	0.641588	−5.04694	−71.3901	
C	a	1.30261	0.724458	−35.0161	304.622	0.9703
	b	−0.855310	−0.410820	−15.5344	−79.1305	
	c	−0.130960	−1.23119	−27.0593	−583.832	
	d	−0.629210	2.86155	4.27835	262.894	
D	a	0.525980	3.50199	−19.7607	421.421	0.9640
	b	−1.30842	2.32861	−12.8615	133.764	
	c	−0.752890	−2.14630	−59.2673	−1036.31	
	d	0.717744	0.403253	−9.08194	−204.396	
Whole sample	a	0.598743	3.00445	−19.2314	436.502	0.9634
	b	−1.11010	1.24458	−10.4805	135.008	
	c	−0.156000	−2.22269	−29.6928	−629.420	
	d	0.326827	0.567390	−6.36708	−116.051	
Case 4—3 earthquakes (0.8526, 1.0000, 0.8526)						
A	a	0.325602	1.21251	−9.27148	294.704	0.9745
	b	−1.12309	−0.262890	−8.89880	175.776	
	c	0.246589	−2.70809	−23.3440	−574.088	
	d	0.888154	0.139158	−11.1732	−174.328	

Table 5 (*continued*)

Soil type	Parameter	1	2	3	4	r^2
B	*a*	0.323280	3.34779	−10.1176	425.646	0.9775
	b	−1.36746	2.39632	−7.46966	205.456	
	c	0.279430	−2.36622	−25.3048	−574.958	
	d	−0.235010	1.69348	−8.20649	9.63346	
C	*a*	0.964969	0.264882	−22.0157	164.674	0.9732
	b	−0.969950	−0.561220	−13.7973	−87.9457	
	c	0.143483	−1.15691	−23.9456	−510.324	
	d	−1.02396	4.34736	1.00583	413.649	
D	*a*	0.244253	2.03700	−8.84940	319.671	0.9718
	b	−1.70297	2.34737	−10.3658	237.247	
	c	0.101749	−2.39598	−43.9956	−1006.14	
	d	0.860710	2.23049	−20.8311	−117.544	
Whole sample	*a*	0.317794	2.20566	−9.35438	308.947	0.9687
	b	−1.41961	1.60134	−9.28507	202.492	
	c	0.231722	−2.52026	−31.1714	−708.855	
	d	0.359789	1.30362	−13.8678	−22.3576	

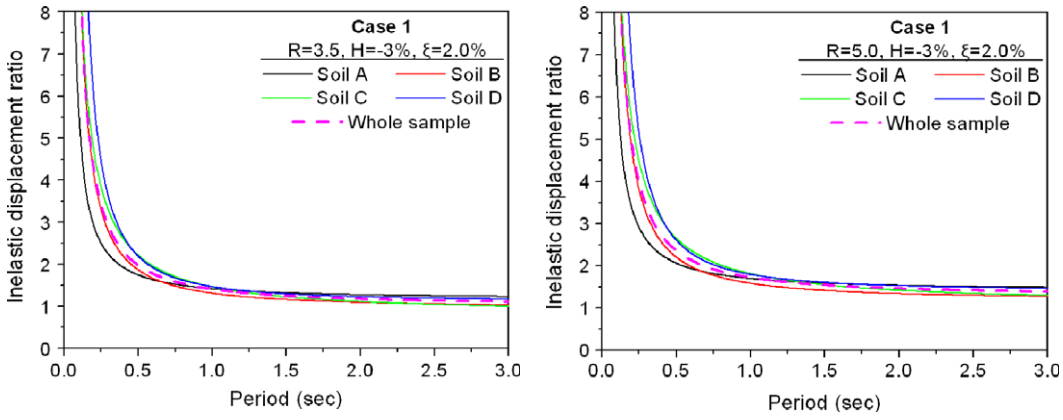

Fig. 6. Influence of local site conditions.

In the case of unacquainted site conditions, one can adopt the appropriate coefficients which correspond to the whole sample.

4. Influence of various parameters and validation

4.1. The influence of basic parameters

This section examines the influence of period of vibration, force reduction factor, site conditions, post-yield stiffness ratio and viscous damping ratio on the inelastic displacement ratios. These aspects are investigated for reasons of completeness as many of them have been also studied by several authors, but in the most cases separately and seldom simultaneously. However, this section emphasizes the effect of repeated earthquakes directly on the inelastic displacement ratios, a phenomenon which has not been studied in the past.

The influence of the viscous damping ratio ξ appears in Fig. 5. It is evident that the increase of the viscous damping ratio always leads to an inappreciable increase of the inelastic displacement ratios. This behavior can be generalized for any soil type, force reduction factor and post-yield stiffness ratio. Therefore, the influence of the viscous damping ratio can be ignored for the estimation of the inelastic displacement ratios. The influence of soil types is typically shown in Fig. 6. It is evident that the inelastic displacement ratios are not significantly affected by local site conditions and can be practically neglected. This characteristic is in agreement with the observations of Miranda [7].

Fig. 7 shows the influence of post-yield stiffness ratio. It is evident that the decrease of this ratio leads to a significantly higher inelastic displacement ratio value and vice versa. This behavior is intense not only for single seismic events but also for a sequence of earthquakes, especially in the case of softening post-elastic behavior. Force reduction factors affect the inelastic displacement ratios, as shown in Fig. 8. It is evident that the increase of R factors always leads to increased inelastic displacement ratio values. Finally, as one can observe from Figs. 5–8, the inelastic displacement ratios are extremely dependent on the structural period of vibration, in any case.

Concluding this section, it should be noted that despite the observed influence of the most critical parameters, i.e. post-yield stiffness ratio, force reduction factors and structural period on the inelastic displacement ratios, there are many seismic design codes which ignore them in the estimations.

4.2. Inelastic displacement ratios for multiple earthquakes and validation

The main objective of this paper has to do with the quantification of the seismic sequence effect directly on the inelastic displacement ratios and not to just underline this observable fact. This objective can be simply achieved using Eq. (10) and Table 5 for the sequence of two or three earthquakes (*Cases* 2–4). This section examines a representative numerical example to illustrate the proposed method and demonstrate its capabilities, focusing on the multiple earthquake influence. Furthermore, the proposed empirical expression is verified with the aid of comparisons against 'exact' dynamic inelastic analyses.

The seismic inelastic behavior of typical steel structures is examined in the following. The majority of seismic codes proposes a viscous damping ratio equal to $\xi = 2\%$ for these structures. The post-yield stiffness may typically vary from −3% to 3%,

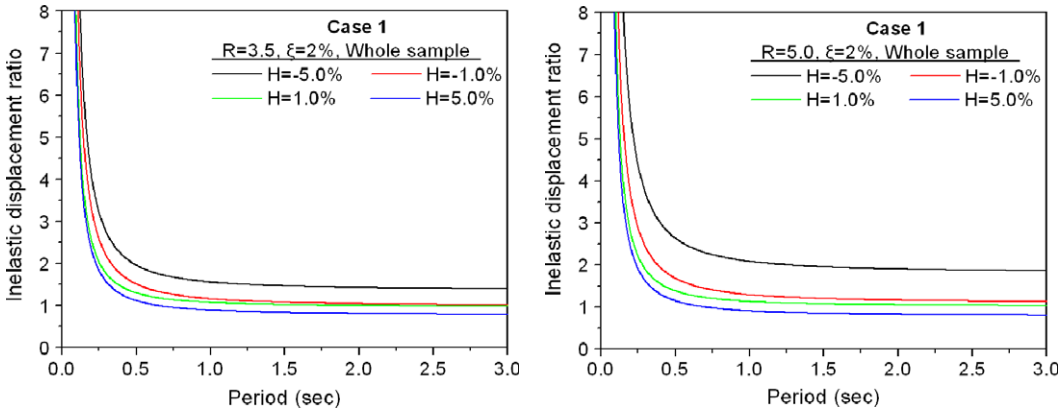

Fig. 7. Influence of post-yield stiffness ratio.

where negative values are frequently present in multi-storey steel buildings including geometrical nonlinearities, while low-rise steel buildings usually exhibit hardening post-elastic behavior. Without loss of generality, the value of $H = -3\%$ is adopted here and soil type A site conditions are assumed. For comparison reasons with the proposed method, mean values from the 'exact' dynamic inelastic analysis using the abovementioned 28 seismic records of Table 1 and values from FEMA356 [32] provisions are also used. According to FEMA356 [32] (Section 3.3.1.3), and for periods $T \geq T_S$, the value of inelastic displacement does not need to be larger than the value derived from the elastic spectrum (equal displacement rule). The characteristic period T_S is typically equal to 1.0 s for soil type A. For very stiff structures, i.e. $T < 0.1$ s, the inelastic displacement ratio is equal to 1.5, while linear interpolation can be used to calculate it for intermediate values of the period. Fig. 9 shows the inelastic displacement ratio spectra, where it is evident that the proposed method closely follows the mean values of 'exact' dynamic inelastic analyses. On the other hand, FEMA356 [32] generally underestimates the 'exact' values, even for Case 1 ('design earthquake') and R equal to 3.5 or 5.0. Additionally, it should be noted that the majority of seismic codes and standards, e.g., Section 4.3.4 of EC8 [24], Section 3.1.1.3 of Greek Seismic Code EAK2000 [33], for medium to long periods (say, 1.0 s to 3.0 s), adopt the abovementioned non-conservative 'equal displacement rule'. This drawback is more pronounced for the case of a seismic sequence.

Eq. (10) can also be used to determine the relative increment (RI) of the inelastic displacement ratio between the multiple earthquakes and the original single events. For typical steel structures and *Cases* (1, 4), the RI can be given by

$$RI_{(1,4)} = \left(\frac{Case\ 4}{Case 1} - 1\right) = \left(\frac{1 + 0.8932\left(\frac{R-1}{R}\right)\left(T^{-0.7032} + R^{0.3761} + 1.069\right)}{1 + 0.3511\left(\frac{R-1}{R}\right)\left(T^{-1.199} + R^{0.7642} - 1.951\right)} - 1\right) \quad (15)$$

where the various parameters are quantified by Eqs. (11)–(14) and Table 5. Similar expressions can be provided for any possible combination of local site conditions, seismic sequence, critical damping and post-yield stiffness ratios. Fig. 10(a) shows the RI where the displacement demands for *Case* 4 and for medium to long periods (say, 1.0–3.0 s) appear to be increased by 100% or more with respect to those obtained for the corresponding single earthquakes. Another useful result can be obtained by comparison of the response to frequent/smaller earthquakes with that to the single 'design earthquake'. Thus, examining the RI for *Cases* (1, 2) and (1, 3), one has

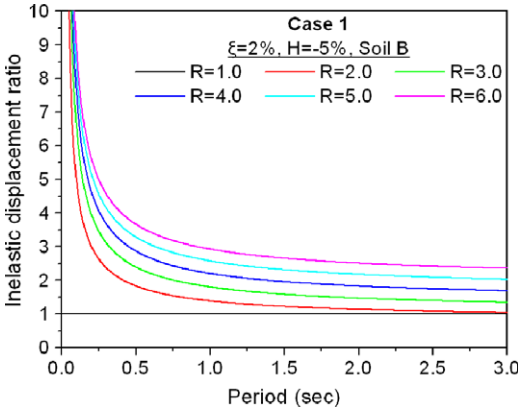

Fig. 8. Influence of force reduction factors.

$$RI_{(1,2)} = \left(\frac{Case\ 2}{Case\ 1} - 1\right) = \left(\frac{1 + 0.7223\left(\frac{0.8526\cdot R-1}{0.8526\cdot R}\right)\left(T^{-0.8604} + (0.8526\cdot R)^{0.4657} + 0.5385\right)}{1 + 0.3511\left(\frac{R-1}{R}\right)\left(T^{-1.199} + R^{0.7642} - 1.951\right)} - 1\right) \quad (16)$$

and

$$RI_{(1,3)} = \left(\frac{Case\ 3}{Case\ 1} - 1\right) = \left(\frac{1 + 5.4147\left(\frac{0.7767\cdot R-1}{0.7767\cdot R}\right)\left(T^{-0.0748} + (0.7767\cdot R)^{-0.0058} - 1.242\right)}{1 + 0.3511\left(\frac{R-1}{R}\right)\left(T^{-1.199} + R^{0.7642} - 1.951\right)} - 1\right). \quad (17)$$

It should be noted that since the design is traditionally based on strength demands, the R factors for the numerators of the above expressions should be multiplied by 0.8526 (*Case* 2—Eq. (8)) and 0.7767 (*Case* 3—Eq. (9)). On the other hand, the 'exact' dynamic inelastic mean values results are determined for the 26 ground motions of Table 1, which are also multiplied with the factors of Eqs. (8) and (9). Fig. 10(b), (c) show the RI spectra of Eqs. (16) *and* (17), respectively, and indicate that frequent/smaller earthquakes require, in any case, increased displacement demands in comparison with the 'design earthquake'. In this example, the displacement demands for medium to long periods (say, 1.0–3.0 s) and for *Cases* 2 and 3 appear to increase by 65% and 90% or more, respectively, with respect to that obtained for the corresponding single earthquakes. Therefore, frequent/smaller earthquakes require, in any case, increased displacement demands in comparison with the 'design earthquake'. This characteristic is

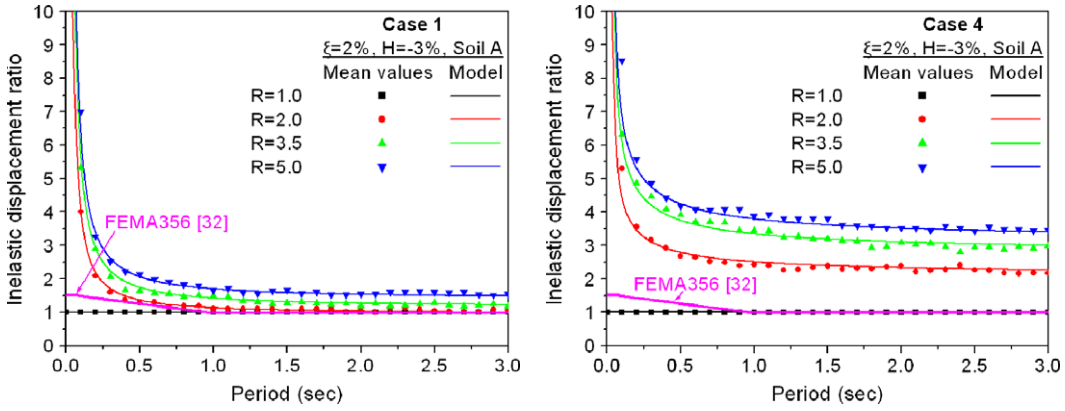

Fig. 9. Efficiency of the proposed model in comparison with FEMA356 [32] provisions.

very important and should be taken into account in the seismic design of structures in order to, for example, avoid collapse due to excessive relative movements of superstructures (decks) for bridges, or reduce the catastrophic damage due to pounding of adjacent buildings, etc. Furthermore, this characteristic should be also taken into account in Displacement-Based Design, since this method requires the 'accurate' estimation of displacements.

The presented numerical example shows that the proposed method gives good results in comparison with the mean values of 'exact' dynamic inelastic analyses. The proposed method can also provide, in any case, the correlation factor, r^2, which describes the degree of relationship between the 'exact' mean values results (from dynamic inelastic analyses) and the model results (from proposed empirical expressions). The best correlation between the 'exact' and the model arrays corresponds to $r^2 = 1.0$, while irrelevant arrays lead to small values for this factor. The global correlation factor of the proposed method for the whole number of 5,644,800 analyses is equal to 0.9508. It should be noted that Table 5, which can be generally used to apply the proposed method, provides the correlation factors for every case under consideration. The importance of graphing data and the effect of outliers on the statistical properties of a dataset should also be noticed. For example, Anscombe [34] presented four simple datasets, which had identical statistical properties (mean values, standard deviation, correlation factor, etc.), but they were found to be very different when inspected graphically. Furthermore, given the uncertainties associated with ground motions, there is a scatter in the estimated seismic demands of a structure [35]. For these reasons, Fig. 11 was constructed to show the inelastic displacement ratio for *Cases* 1 and 4 and compare the 'exact' dynamic inelastic analyses results (scatter data without averaging) with the proposed model, which is based on Eq. (10). It is obvious that the model results obtained from this study are in good agreement with those obtained from the well-accepted dynamic inelastic analyses, thus confirming the validity of the proposed method.

5. Comments on the proposed method

As was previously mentioned, real sequences of seismic events are not examined here since they present dissimilar characteristics, making the analysis extremely complex and not leading to transpicuous and practically useful conclusions. For example, one can mention the aforesaid Coalinga earthquake sequence, where the second examined earthquake is more critical than the first, despite its smaller magnitude. Generally, it should be noted that the inelastic displacement ratio depends on the characteristics of the seismic motions. However, the influence of these features is eliminated, despite the reproducing of related ground motions, due to

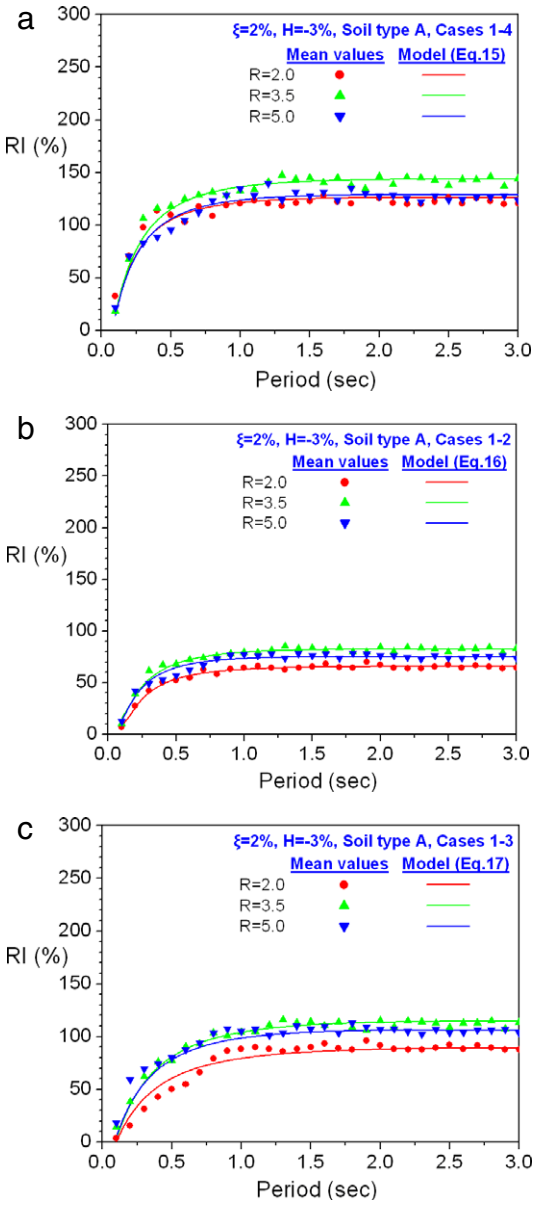

Fig. 10. Relative increment of the inelastic displacement ratio for frequent/smaller earthquakes.

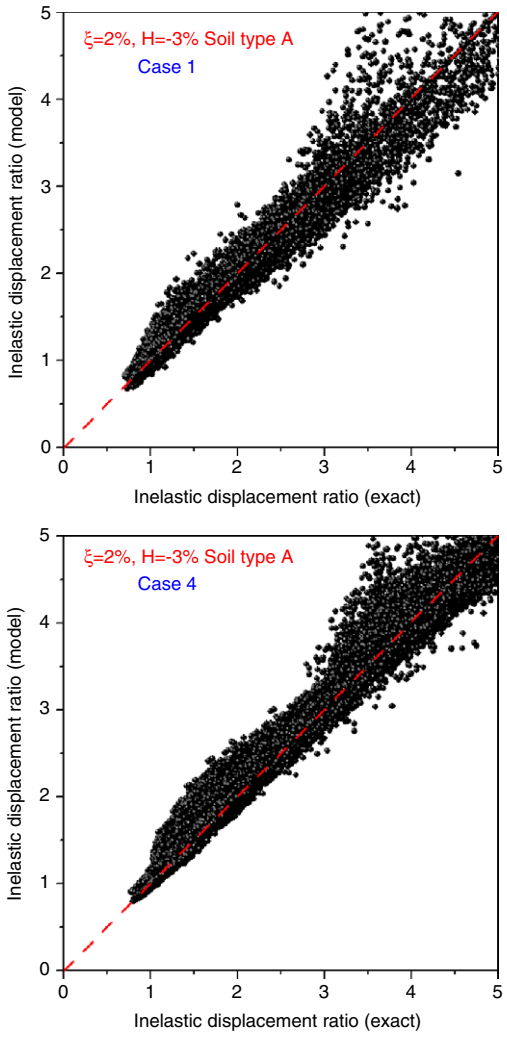

Fig. 11. Comparison of proposed model (Eq. (10)) with 'exact' scatter data—*Cases* 1, 4.

- examination of an adequate number of seismic events (112 severe ground motions in this work),
- the general uncertainties associated with ground motions, and
- the traditional averaging (mean values) of dynamic inelastic analysis results.

Additionally, the adopted cases of seismic sequence are absolutely compatible with the traditional Engineering Seismology [29, 31]. Furthermore, *Cases* 2 and 3 should be applied, in any case, using the aforementioned appropriate factors of Eqs. (8) and (9) since it is obviously unrealistic to consider two or three times the 'design earthquake'. Thus, *Cases* 2 and 3 are exclusively adopted to examine the influence of smaller/frequent earthquakes on structures in comparison with the 'design earthquake'. Finally, it seems to be impractical to examine isolated 'design earthquakes'. One can mention numerous earthquakes with strong foreshocks and aftershocks, e.g., the Mammoth Lakes earthquake (1980/5/25) for which the main shock of magnitude $M_L = 6.2$, was followed by five aftershocks with magnitudes $M_L = 5.7$–6.1, in the next two days. In these cases, the damage accumulation is continuous and hence, due to lack of time, any rehabilitation action is impractical.

It should be noted that the proposed empirical expression (Eq. (10)) is simple and unique for each combination of the factors under consideration, i.e., T, R, ξ, H, soil type and seismic sequence. Furthermore, the proposed empirical relation satisfies the following fundamental condition:

$$\text{Inelastic displacement ratio}\,(T, R) \overset{T\to 0}{=} \infty, \tag{18}$$

which means that, irrespective of the value of their force reduction factor, very stiff structures should be designed elastically. This is because the yield displacement u_y tends to zero, and even a small decrease in strength that retains the structure in the elastic range leads to a very large inelastic displacement. Therefore, very stiff structures should be designed as absolutely elastic systems. Furthermore, Eq. (10) also satisfies the fundamental condition

$$\text{Inelastic displacement ratio}\,(T, R) \overset{R\to 1}{=} 1. \tag{19}$$

This obvious condition results from the definition of the force reduction factor, which indicates that, irrespective of their period, structures behaving elastically should be designed without reduction of their strength.

Various researchers, e.g., Veletsos and Newmark [5] as well as seismic codes and standards, e.g., EC8 [27], FEMA356 [32], EAK2000 [33] predicate that flexible structures (say $T > 1.0$ s), present maximum inelastic displacements equal to the corresponding elastic displacement demands (equal displacement rule). Therefore, according to this thought, for every seismic motion, the inelastic strength demand is equal to the elastic strength demand divided by the ductility, and therefore (see Eq. (5)), the following relationship holds:

$$\text{Inelastic displacement ratio}\,(T, R) \overset{T>1.0\text{ s}}{\approx} 1.0. \tag{20}$$

According to the authors' opinion, the validity of this condition is uncertain in the case of repeated earthquakes. It should be recognized that the maximum relative displacement tends towards the maximum ground displacement for elastic flexible systems. In this case, the structure has a practically insignificant total displacement, while the relative displacement is almost identical to the maximum ground displacement. For a single seismic event, inelastic flexible systems have also practically insignificant total displacement, while the relative displacement is almost identical to the maximum ground displacement too. However, the main difference between them has to do with their permanent displacements: that is, elastic flexible systems present zero permanent displacements, in any case, while inelastic flexible systems present permanent displacements, which are almost equal to the maximum ground displacements for small values of yield displacements (e.g., $R > 4.0$) and single seismic events. Nevertheless, for any other oncoming ground motion, e.g., typical foreshocks, permanent displacements and inelastic displacement ratios are cumulated and the validity of Eq. (20) is lost.

For example, as shown in Fig. 9 for flexible systems (say, $T = 3.0$ s), the inelastic displacement ratios become greater than 1.0 for every case under consideration. This characteristic is more pronounced in the case of a seismic sequence (*Case* 4) where the inelastic displacement ratios appear to be increased by 100% or more with respect to that obtained for the corresponding single earthquakes. As shown in this typical example, the larger the R factor, the higher the inelastic displacement ratio.

In conclusion, this paper quantifies the seismic sequence effect directly in the form of inelastic displacement ratios (see Table 5 and Eqs. (15)–(17)). Furthermore, it was found that repeated frequent/smaller earthquakes lead to similar results coming from the "design earthquake". Therefore, these results can affect, in a direct or indirect manner, the performance-based seismic design, which should be revised according to those results.

6. Conclusions

This paper proposes a new method for evaluating the inelastic displacement ratios of SDOF systems on the basis of empirical expressions obtained after extensive parametric studies. The influence of period of vibration, force reduction factor, soil type conditions, post-yield stiffness ratio (hardening and softening) and viscous damping ratio is carefully examined and discussed. The main innovation of this work has to do with the quantification of the seismic sequence effect directly onto displacement demands, a problem which has not been studied in the past. A detailed study of the influence of the various parameters of the problem on the inelastic displacement ratio leads to the following conclusions:

1. The increase of force reduction factors always leads to an increase of the inelastic displacement ratio and vice versa. Furthermore, these ratio values are extremely dependent on the structural period of the SDOF system, especially in the short-period range, say up to 0.5 s. In this case, the lower the period, the higher the inelastic displacement ratio. Additionally, the decrease of post-yield stiffness ratio leads to higher displacement demands and vice versa. This effect is more pronounced for negative values of this parameter, i.e., for softening behavior.
2. The local site conditions and the viscous damping ratio influence the inelastic displacement ratio slightly, and can be practically ignored.
3. This paper quantifies the seismic sequence effect directly on the inelastic displacement ratio and does not just underline this observable fact. Multiple earthquakes require increased displacement demands in comparison with single seismic events ('design earthquake'). Thus, in many cases, the inelastic displacement ratio appears to be increased by 100% or more with respect to that obtained for the corresponding single earthquakes. This characteristic is very important and should be taken into account for the seismic design of structures either by the conventional force-based method or especially by the more recent displacement-based design method, which requires a high accuracy estimation of displacements.
4. The traditional seismic design procedure, which is essentially based on the isolated 'design earthquake', should be reconsidered.
5. Corresponding theoretical background examining all the parameters and characteristics of multi degree of freedom (MDOF) systems as well as appropriate empirical expressions for their inelastic displacement ratios are currently being derived, and will be presented in a future paper.

References

[1] Applied Technology Council (ATC). ATC-40: Seismic evaluation and retrofit of concrete buildings. California; 1996.
[2] Chopra AK, Goel R. Evaluation of NSP to estimate seismic deformations: SDF systems. J Struct Eng 2000;126(4):482–90.
[3] Chopra AK, Goel RK. A modal pushover analysis procedure for estimating seismic demands for buildings. Earthq Eng Struct Dyn 2002;31(3):561–82.
[4] Veletsos AS. Maximum deformations of certain nonlinear systems. In: Proceedings of 4th world conf. on earthquake engineering. Chilean Association on Seismic and Earthquake Engineering. Vol. II, A4-155–A4-170, 1969.
[5] Veletsos AS, Newmark NM. Effect of inelastic behavior on the response of simple systems to earthquake motions. In: Proceedings of 2nd world conf. on earthquake engineering. Tokyo (Japan): Science Council of Japan; 1960. p. 895–912.
[6] Clough RW. Effect of stiffness degradation on earthquake ductility requirements. Rep. no. SEMM 66-16. Berkeley (CA): Dept. of Civil Engineering, Univ. of California at Berkeley; 1966.
[7] Miranda E. Inelastic displacement ratios for structures on firm sites. J Struct Eng 2000;126(10):1150–9.
[8] Decanini LD, Liberatore L, Mollaioli F. Characterization of displacement demand for elastic and inelastic SDOF systems. Soil Dyn Earthq Eng 2003;23: 455–71.
[9] Ruiz-Garcia J, Miranda E. Inelastic displacement ratios for evaluation of existing structures. Earthq Eng Struct Dyn 2003;32:1237–58.
[10] Ruiz-Garcia J, Miranda E. Inelastic displacement ratios for design of structures on soft soil sites. J Struct Eng 2004;130(12):2051–61.
[11] Chopra AK, Chintanapakdee C. Inelastic deformation ratios for design and evaluation of structures: Single-degree-of-freedom bilinear systems. J Struct Eng 2004;130(9):1309–19.
[12] Akkar SD, Miranda E. Statistical evaluation of approximate methods for estimating maximum deformation demands on existing structures. J Struct Eng 2005;131(1):160–72.
[13] Ruiz-Garcia J, Miranda E. Inelastic displacement ratios for evaluation of structures built on soft soil sites. Earthq Eng Struct Dyn 2006;35(6):679–94.
[14] Mollaioli F, Bruno S. Influence of site effects on inelastic displacement ratios for SDOF and MDOF systems. Comput Math Appl 2008;55:184–207.
[15] Chenouda M, Ayoub A. Inelastic displacement ratios of degrading systems. J Struct Eng 2008;134(6):1030–45.
[16] Qi X, Moehle JP. Displacement design approach for reinforced concrete structures subjected to earthquakes. Rep. no. EERC-91/02, Berkeley (CA): Earthquake Engineering Research Center, Univ. of California at Berkeley; 1991.
[17] Whittaker A, Constantinou M, Tsopelas P. Displacement estimates for performance-based seismic design. J Struct Eng 1998;124(8):905–12.
[18] Amadio C, Fragiacomo M, Rajgelj S. The effects of repeated earthquake ground motions on the non-linear response of SDOF systems. Earthq Eng Struct Dyn 2003;32:291–308.
[19] Hatzigeorgiou GD. Site-dependent force reduction factors including the effect of seismic sequence. Bull Earthq Eng. Under review.
[20] Fajfar P. Equivalent ductility factors taking into account low-cycle fatigue. Earthq Eng Struct Dyn 1992;21:837–48.
[21] Cosenza E, Manfredi G. Seismic design based on low cycle fatigue criteria. In: Proceedings of XI world conference on earthquake engineering (CD). 1996.
[22] Chai YH. Incorporating low-cycle fatigue model into duration-dependent inelastic design spectra. Earthq Eng Struct Dyn 2004;34:83–96.
[23] Teran-Gilmore A, Bahena-Arredondo N. Cumulative ductility spectra for seismic design of ductile structures subjected to long duration motions: Concept and theoretical background. J Earthq Eng 2008;12(1):152–72.
[24] Chopra A. Dynamics of structures: Theory and applications to earthquake engineering. 3rd ed. New Jersey: Prentice Hall Inc.; 2006.
[25] Boore DM. Some notes concerning the determination of shear-wave velocity and attenuation. In: Proceedings of geophysical techniques for site and material characterization. 1993. p. 129-34.
[26] Pacific Earthquake Engineering Research Center. PEER strong motion database. [accessed 01.03.09] http://peer.berkeley.edu/smcat.
[27] European Committee for Standardization. Eurocode 8: Design of structures for earthquake resistance. 2003.
[28] Elnashai AS, Bommer JJ, Martinez-Pereira A. Engineering implications of strong-motion records from recent earthquakes. In: Proceedings of 11th European conference on earthquake engineering. 1998.
[29] Gutenberg B, Richter CF. Seismicity of the earth and associated phenomena. 2nd ed. Princeton (NJ): Princeton University Press; 1954.
[30] Chouhan RKS, Srivastava VK. Global Variation of b in the Gutenberg Richter's relation $\mathrm{Log}N = a - bM$ with depth. Pure Appl Geophys 1970;82(1):124–32.
[31] Joyner WB, Boore DM. Prediction of earthquake response spectra. USGS Open-file report. 1982. p. 82–977.
[32] Federal Emergency Management Agency. Prestandard and commentary for the seismic rehabilitation of buildings. Rep. FEMA 356, Washington (DC); 2000.
[33] Greek Seismic Code. EAK 2000. Technical Chamber of Greece, Greek Government Journal—FEK 2184/B/99, Athens (Greece); 2000.
[34] Anscombe FJ. Graphs in statistical analysis. Amer Statist 1973;27:17–21.
[35] Lam N, Wilson J, Hutchinson G. The ductility reduction factor in the seismic design of buildings. Earthq Eng Struct Dyn 1998;27:749–69.